Energy & Environmental Science

Cite this: *Energy Environ. Sci.*, 2011, **4**, 4246

www.rsc.org/ees

PAPER

Hydrogen evolution at polarised liquid/liquid interfaces catalyzed by molybdenum disulfide†

Imren Hatay,‡[a] Pei Yu Ge,[a] Heron Vrubel,[b] Xile Hu[b] and Hubert H. Girault*[a]

Received 22nd June 2011, Accepted 27th July 2011
DOI: 10.1039/c1ee01996a

Molybdenum disulfide microparticles in suspension in an aqueous acidic solution adsorb at the interface with an organic electrolyte solution containing the reducing agent, decamethylferrocene, to catalyse hydrogen evolution. This catalytic process has been investigated by voltammetry at the water/1,2-dichloroethane interface and by biphasic reactions monitored by gas chromatography and UV-visible spectroscopy.

1. Introduction

Natural photosynthesis occurs in biological membranes that can be viewed at thin organic liquid membranes separating two aqueous solutions. The thylakoid membrane is a physical barrier separating the production of protons on one side associated with the oxidation of water and the production of NADPH on the other side. With the aim of developing artificial photosynthetic systems based on the use of an organic liquid membrane, one can envisage a system with two photosystems on either side of this membrane able to oxidize water and reduce protons, respectively. To carry out charge transfer reactions at a liquid/liquid interface, it is important to consider the electrochemical aspects. Indeed, the Interface between Two Immiscible Electrolyte Solutions (ITIES) can be polarized as a classical metal or a semiconductor/electrolyte interface, but in this case the potential drop between the two phases takes place across two back-to-back Gouy–Chapman diffuse layers. By controlling electrochemically the potential difference across this interface, it is possible to apply classical electrochemical methods such as voltammetry to study the different charge transfer reactions that can take place, namely ion transfers, assisted ion transfers such as acid–base interfacial reactions and heterogeneous electron transfer reactions between redox couples, one being hydrophilic and the other being lipophilic.[1] The ITIES presents some interesting features for studying reactions of interest for energy research, and for example adsorbed molecular or metallic nanoparticles catalysts can drive oxygen reduction at the interface. The molecular catalysts studied include cobalt[2–6] and free base porphyrins,[7,8] whereas metallic nanoparticles were made of platinum.[9] Protons can also be reduced at the ITIES to produce hydrogen if an organic reducing agent such as cobaltocene[10] or decamethylferrocene (DMFc)[11] is used in the organic phase. We have recently shown that hydrogen production at the ITIES can be catalyzed by the *in situ* reduction of metallic salts forming adsorbed nanoparticles of platinum or palladium.[12]

In biological systems, hydrogen evolution occurs with enzymes such as hydrogenases and nitrogenases. The catalytically active site of these enzymes has both metal atoms, such as Fe, Ni, Mo, and sulfur atoms. In this context, inorganic metal sulfide MoS_2 catalysts, which have a structure somewhat analogous to the nitrogenase active site, have extensively been investigated for the Hydrogen Evolution Reaction (HER) following the pioneering work of Tributsch and Bennett in 1977.[13] In 1986, Nidola and

[a]*Laboratoire d'Electrochimie Phyique et Analytiqu, Station 6, Ecole Polytechnique Fédédrale de Lausanne, Lausanne, Swizerland. E-mail: Hubert.Girault@epfl.ch; Fax: +41 693 3667; Tel: +41 693 3145*
[b]*Laboratory of Inorganic Synthesis and Catalysis, Ecole Polytechnique Fédédrale de Lausanne, BCH 3305 1015 Lausanne, Switzerland. E-mail: xile.hu@epfl.ch; Fax: +41 (0)216939305; Tel: +41 (0)21 6939781*

† Electronic supplementary information (ESI) available: The video of hydrogen evolution, the characterization of MoS_2 microparticles by electron diffraction analysis, XPS and TEM, the molar extinction coefficient of $DMFc^+$ and fitting curves of Fig. 5. See DOI: 10.1039/c1ee01996a

‡ Present address: Selcuk University, Department of Chemistry, 42031 Konya, Turkey.

Broader context

Hydrogen evolution reactions (HER) can be catalyzed efficiently by molybdenum disulfide microparticles at polarized interfaces between an aqueous acidic solution and an organic solution containing an electron donor, *e.g.*, decamethylferrocene (DMFc). This work opens a new perspective to the investigation of other triphasic systems for the production of hydrogen without noble metal catalysts.

Schira[14] had reported that the HER activity and the stability of a NiS coating increased in the presence of MoS_2 due to the enhancement of the "true surface area". Another HER study on MoS_2 (1991) was explored by Sobczynski,[15] who found that hydrogen was produced from acidic V^{+2} solutions using MoS_2 supported on porous silica. More recently, it has been shown that MoS_2 single crystals and nanoparticles exhibit high activity for HER, and the catalysis occurs at the edge sites.[16–18] In addition, MoS_2 colloids have been used as HER catalysts in photolytic hydrogen production based on CdS.[19] The MoS_2 catalysts are interesting because they are relatively cheap and abundant.

Herein, we have studied the catalytic role of commercial MoS_2 microparticles in HER at polarized liquid/liquid interfaces between an aqueous acidic solution and a solution of decamethylferrocene (DMFc) acting as a molecular electron donor in the organic phase. This catalytic process is studied by voltammetry at the ITIES and two-phase reactions.

2. Experimental

Decamethylferrocene (DMFc, 99%) was obtained from Alfa Aesar and purified by vacuum sublimation at 140 °C.[20] Molybdenum(IV) sulfide (MoS_2) with the average particle size of 6 μm (max 40 μm) was purchased from Aldrich (Catalogue number: 69860). XPS spectra show a binding energy of 228.5 eV for Mo $3d_{5/2}$, indicating a +4 oxidation state for the Mo center and a doublet at energies of 163.5 and 162.3 eV with an area ratio of 1 : 2 corresponding, respectively, to the levels S $2p_{3/2}$ and S $2p_{1/2}$ of the S^{2-} ligands (Fig. S1†). TEM analysis shows a layered organization of the solid while electron diffraction experiments confirm a microcrystalline structure for this commercial sample (Fig. S2†).

Lithium tetrakis(pentafluorophenyl)borate (LiTB) diethyl etherate and tetrafluoroboric acid (HBF_4) (54% in diethyl ether) were purchased from Aldrich. Tetraethylammonium chloride (TEACl, ≥98%), bis(triphenylphosphoranylidene)ammonium chloride (BACl, ≥98%), and 1,2-dichloroethane (1,2-DCE, ≥ 99.8%) were obtained from Fluka. Hydrochloric acid (HCl, 32%) was purchased from Merck. Bis(triphenylphosphoranylidene)-ammonium tetrakis(pentafluorophenyl)borate (BATB) was prepared by metathesis as reported previously.[21] All aqueous solutions were prepared with ultrapure water (18.2 MΩ cm).

The voltammetry measurements at the water/1,2-DCE interface were performed in a four-electrode configuration using a PGSTAT potentiostat (Eco-Chemie, Netherlands) in a glove box under anaerobic conditions. Two platinum counter-electrodes were positioned in the aqueous and organic phases, respectively, to supply the current flow. The external potential was applied by means of two reference electrodes, silver/silver chloride (Ag/AgCl), which were connected to the aqueous and 1,2-DCE phases, respectively, *via* a Luggin capillary as illustrated in Fig. 1. The area of the liquid/liquid interface was 1.53 cm^2. The Galvani potential difference across the interface was determined by assuming the formal ion-transfer potential of a tetraethylammonium cation (TEA^+) to be 0.019 V.[22]

Two-phase reactions were performed in a small glass flask with mechanical stirring in a glove box under anaerobic conditions. The flask was filled first with 2 mL of the 1,2-DCE solution containing 5 mM DMFc, followed by the addition of 2 mL of an aqueous solution containing 100 mM HCl in the presence and absence of MoS_2 (0.625 μmol) particles. Two salts sharing a common anion (TB^-), LiTB and BATB, were added at the same concentration of 10 mM to the aqueous and 1,2-DCE phases, respectively. After stirring the phases, the headspace gas phase was analyzed by gas chromatography (Perkin-Elmer, Clarus 500) using a thermal conductivity detector and argon as the carrier gas. Hydrogen quantification was determined by calibration using standard samples of H_2 in nitrogen. The hydrogen amount was also calculated from the concentration of $DMFc^+$ measured by UV-vis spectroscopy. In this case, a molar extinction coefficient of $DMFc^+$ in 1,2-DCE was determined by using $DMFcBF_4$ prepared by mixing DMFc and HBF_4 (strong acid) for 24 hours under stirring conditions (Fig. S3†). The value obtained at 779 nm was $\varepsilon = 0.632\ mM^{-1}\ cm^{-1}$.

Fig. 1 Four electrode cell containing 1 mM DMFc in the 1,2-DCE phase (bottom) and 0.5 mM MoS_2 (top) in water using the electrochemical cell composition shown in Scheme 1.

3. Results and discussion

Electrochemical measurements at the water/1,2-DCE interface were performed by four-electrode voltammetry using the electrochemical cell composition in Scheme 1 in a cell as shown in Fig. 1. Fig. 2a compares the cyclic voltammograms (CVs) obtained for the blank cell containing only the supporting electrolytes (dotted line), in the presence of only DMFc in the 1,2-DCE phase (solid line) and in the presence of both DMFc in 1,2-DCE and MoS_2 as a suspension in the aqueous phase (dashed line) under anaerobic conditions. The positive and negative potential limits of the blank CV stem from the transfer of H^+ and Cl^- from the water to the organic phase, respectively. The presence of only DMFc in 1,2-DCE results in a small current increase at positive potentials (solid line).

As reported recently,[11] this current increase can be attributed to the assisted proton transfer reaction by DMFc from the water to the organic phase, leading to the formation of decamethylferrocene hydride $(DMFc–H)^+$.

The formation of the hydride form was confirmed by NMR analysis of a solution of DMFc in 1,2-DCE containing an organic acid, *e.g.*, HTB. This assisted proton transfer reaction is

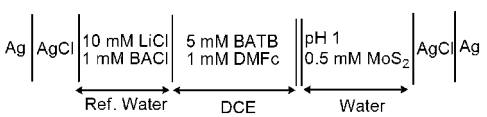

Scheme 1 Electrochemical cell composition used in Fig. 1.

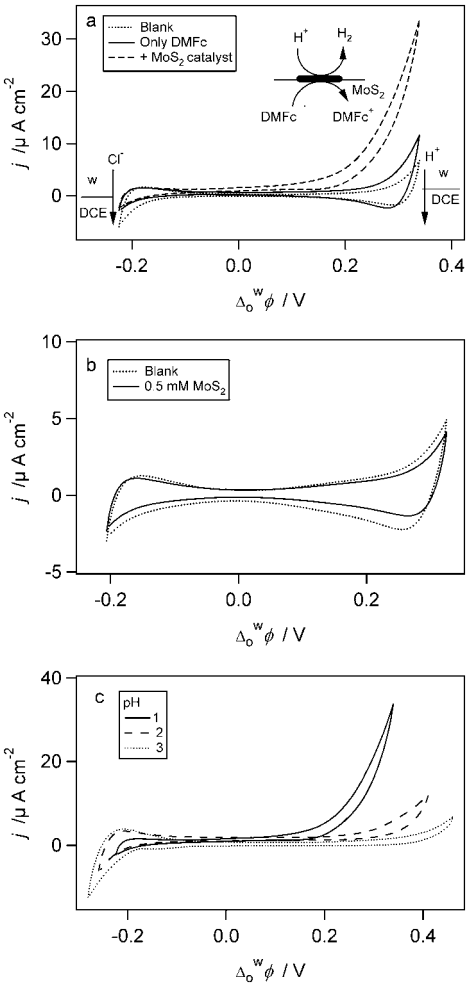

Fig. 2 Cyclic voltammograms using cell 1 under anaerobic conditions at a scan rate of 50 m V s^{-1}. The second scan is compared: (a and b) blank in the absence of both DMFc and MoS_2 (dotted line); (a) with added DMFc in 1,2-DCE (solid line) and both DMFc in 1,2-DCE and MoS_2 in water (dashed line); (b) Fig. 2b: with only added MoS_2 in water; (c) with both DMFc in 1,2-DCE and MoS_2 in water at different pH values: pH = 1 (solid line), pH = 2 (dashed line) and pH = 3 (dotted line).

characterized by the absence of a return peak, indicating that the hydride formation is followed by chemical reactions in the organic phase producing both $DMFc^+$ and hydrogen. The presence of only MoS_2 in the aqueous phase does not give rise to any voltammetric response as compared to the blank CV (Fig. 2b). When the aqueous phase contains a suspension of MoS_2 microparticles in the presence of DMFc in 1,2-DCE, a large positive current can be observed at less positive potentials (dashed line in Fig. 2a) than in the assisted proton transfer process. By analogy with previous studies where Pd or Pt nanoparticles were electrogenerated at the interface, this large current can be attributed to a heterogeneous H_2 production where the aqueous protons are reduced on interfacial MoS_2 particles, also contacting the organic electron donors as schematically represented in the inset of Fig. 2a. This current should not involve the formation of decamethylferrocene hydride but the adsorption of the protons on the MoS_2 particles, likely on the edges. This means that MoS_2 can act as an interfacial electrocatalyst at a polarised liquid/liquid interface able to store at least two electrons. Indeed, it can be seen in Fig. 1 that after a while some MoS_2 particles sediment and adsorb at the interface that loses its mirror appearance. They also adsorb at the three-phase junction, water–1,2-DCE–glass, as can be observed visually from the dark rim on the glass. It is important to note that these particles are soluble neither in the water nor in the organic phase and that the suspension can sediment with time. The voltammograms presented in Fig. 2 were recorded with freshly contacted solutions. The picture in Fig. 1 was taken after a couple of hours to show the sedimentation. Fig. 2c shows the pH dependence where the heterogeneous electron transfer wave shifts about 60 mV pH^{-1}, indicating that the protons are involved in the amperometric response.

The reaction between DMFc and aqueous protons catalyzed by adsorbed MoS_2 particles as investigated by voltammetry can be written as

$$DMFc_{(DCE)} + H^+_{(w)} \xrightarrow{MoS_2} DMFc^+_{(DCE)} + \frac{1}{2}H_{2(g)} \quad (1)$$

The Nernst equation for this heterogeneous electron transfer reaction is[1]

$$\Delta^w_o\phi = \Delta^w_o\phi^0_{HET} + \frac{RT}{F}\ln\left(\frac{a^{DCE}_{DMFc^+} f^{1/2}_{H_2}}{a^{DCE}_{DMFc} a^w_{H^+}}\right) \quad (2)$$

where $\Delta^w_o\phi$ is the Galvani potential difference between the water (w) and the organic phase (o). $\Delta^w_o\phi^o_{HET}$ represents the standard Galvani potential for the heterogeneous electron transfer which is given by

$$\Delta^w_o\phi^0_{HET} = \left[E^0_{DMFc^+/DMFc}\right]^{DCE}_{SHE} - \left[E^0_{H^+/1/2H_2}\right]^{w}_{SHE} \quad (3)$$

where $\left[E^0_{DMFc^+/DMFc^+}\right]^{DCE}_{SHE} = 0.04$ V is the standard redox potential for decamethylferrocene in 1,2-DCE expressed on the aqueous standard hydrogen electrode scale (SHE).[23] This value was obtained by measuring first in 1,2-DCE with respect to ferrocene $\left[E^0_{DMFc^+/DMFc}\right]^{DCE}_{Fc} = -0.60$ V. The standard redox potential of ferrocene in 1,2-DCE but with respect to the aqueous SHE scale was obtained using thermodynamic cycles described previously $\left[E^0_{Fc^+/Fc}\right]^{DCE}_{SHE} = 0.64$ V.[23]

This careful consideration of the redox scales is very important when studying heterogeneous electron transfer reactions in biphasic systems. As can be seen in Fig. 2, the onset for hydrogen evolution is about 0.2 V, *i.e.*, with an overvoltage of only 0.1 V more positive than the standard driving force given by

$$\Delta G_{HET}/F = \Delta^w_o\phi - [\Delta^w_o\phi^0_{HET} + 0.06\ pH] \quad (4)$$

Indeed, the observed current increase shifts with pH approximately 0.06 V pH^{-1}, as shown in Fig. 2c, and as suggested by eqn (4). This shows that the overvoltage for H_2 evolution at soft interfaces is relatively small and comparable to that obtained with MoS_2 modified solid electrodes.[24]

The fact that hydrogen evolution at the ITIES occurs at positive Galvani potential differences and not at negative reducing potentials as on a solid electrode is only due to the convention water *vs.* oil.

This catalytic process was also investigated by two-phase reactions as reported previously.[25] Herein, the distribution Galvani potential difference across the water/1,2-DCE interface is fixed chemically by the distribution of all the ions of the supporting electrolytes. When using LiTB in water, the aqueous protons can be driven to the organic phase and the acid HTB is extracted. As illustrated in Fig. 3, the acidic aqueous phase (100 mM HCl + 10 mM LiTB) and the 1,2-DCE phase containing only 5 mM DMFc in flask 1 and the same but with MoS_2 in flask 2 were mixed and stirred for 1 hour under anaerobic conditions. After these reactions, where the two phases are emulsified mechanically, the microparticles sediment at the bottom of the organic phase on the glass surface.

It should be noted that identical results were obtained by suspending MoS_2 either in the water or in the organic phase, as anyway they are likely to adsorb at the liquid/liquid interface during the emulsification to lower their energy.

The headspace gas above the two liquid phases was analyzed by gas chromatography. As shown in Fig. 4a, the gas chromatograms clearly indicate that the rate of hydrogen evolution increases significantly in the presence of MoS_2 particles. For comparison, after 1 hour stirring and further waiting for the clear separation of two phases (about 1–2 min), the UV-visible analysis of the 1,2-DCE phases separated from the aqueous ones was carried out as presented in Fig. 4b. A freshly prepared DMFc solution in 1,2-DCE is yellow, displaying an absorption band in the UV-visible spectrum at $\lambda_{max} = 425$ nm (dashed line, Fig. 4b). During the two-phase reaction in the absence of MoS_2, the color of the organic phase turns gradually from yellow to green (flask 1, Fig. 3), showing an absorption band at $\lambda_{max} = 779$ nm due to the formation of $DMFc^{+}$[25] (dotted line, Fig. 4b). In the presence of both DMFc and MoS_2, the color of the organic solution turns immediately green (flask 2, Fig. 3). These results confirm that the oxidation of DMFc associated with the hydrogen production is significantly accelerated in the presence of MoS_2 catalysts.

Hydrogen formation can also be monitored visually by a video camera (ESI)†. Herein, a drop of 50 mM DMFc in 1,2-DCE (10 mM BATB) was placed in an aqueous acidic solution containing MoS_2 particles (100 mM HCl + 10 mM LiTB). After a couple of seconds, the formation of the interfacial H_2 gas bubbles can be observed and the droplet color changes from yellow to green, indicating an oxidation of DMFc. It can also be observed that the MoS_2 particles swirl violently at the interface, showing that large Marangoni effects are generated from the chemical reaction. Indeed, it is important to realize that nano/micro-particles do float at liquid/liquid interfaces forming catalytic rafts.[26]

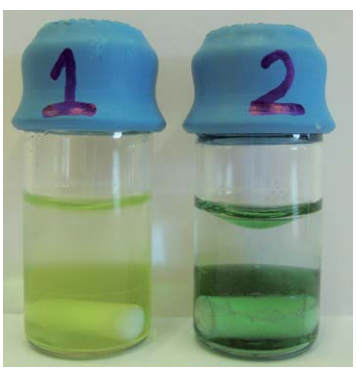

Fig. 3 Two-phase reactions controlled by the TB^- anion after 1 hour shaking: the water phases contain 10 mM LiTB + 100 mM HCl for flask 1 and 10 mM LiTB + 100 mM HCl + 0.625 μmol MoS_2 particles for flask 2; the 1,2-DCE phases contain only 5 mM DMFc for each flask.

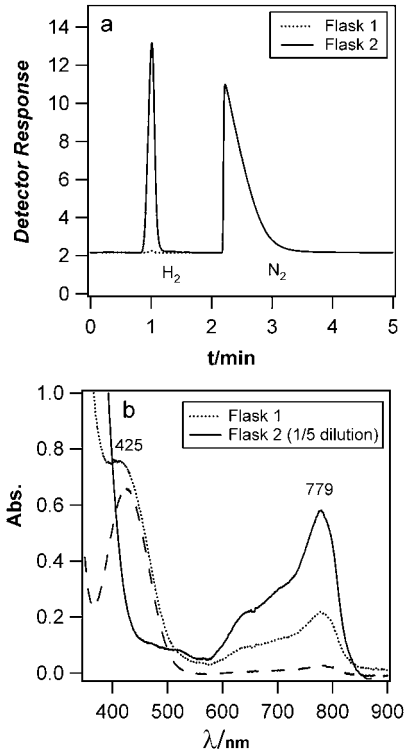

Fig. 4 (a) Gas chromatograms of the headspace gas above the liquids for flasks 1 and 2 and (b) UV-visible absorption spectra of the 1,2-DCE phases separated from flasks 1 and 2 obtained after two-phase reactions illustrated in Fig. 2. A freshly prepared 5 mM DMFc solution in 1,2-DCE is also given for comparison (dashed line).

The biphasic reactions were also performed at different time scales. The amount of hydrogen produced was calculated analyzing the headspace by gas chromatography and from the amount of $DMFc^+$ produced using UV-vis measurements and assuming a stoichiometric reaction (1):

$$DMFc_{(DCE)} + H^+_{(w)} + TB^-_{(w)} \rightarrow DMFc^+_{(DCE)} + TB^-_{(DCE)} + {}^1/_2\, H_{2(g)} \quad (5)$$

As shown in Fig. 5, the results of these two analyses corroborate each other. It can be observed that the formation of hydrogen by DMFc is kinetically a slow process, producing about 0.8 μmol of hydrogen after 24 hours of two-phase reaction. In the presence of both DMFc and MoS_2 particles, the evolution of hydrogen reached the maximum theoretical stoichiometric amount of about 5 μmol after just one hour, limited here by the initial amount of DMFc (10 μmol). This experiment corresponds to a turnover number (TON) of about 16 in 60 minutes.

Assuming that hydrogen evolution reaction is directly proportional to the DMFc concentration in the presence of an excess of protons, the pseudo-first-order reaction rate constants

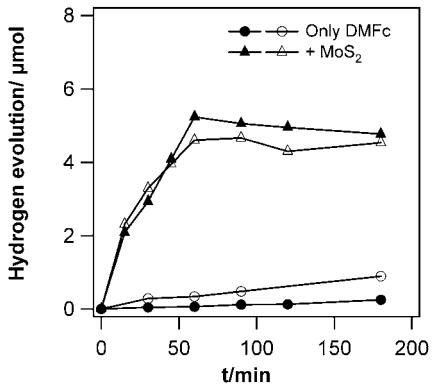

Fig. 5 (a) Hydrogen evolution by DMFc as a function of time (min) in the absence (circles) and presence (triangles) of MoS_2 catalysts. The evolved hydrogen calculated from the UV-visible spectra of the 1,2-DCE phases (open circles and triangles) and gas chromatography (closed circles and triangles).

can be calculated approximately as 1×10^{-5} and 7.2×10^{-8} M min^{-1} with and without MoS_2, respectively (see Fig. S4†). This result shows that the presence of MoS_2 particles results in an about 140 times increased hydrogen formation rate.

In the case of the biphasic reaction carried out under stirring conditions, it is impossible to determine the locus of the reaction and to differentiate a truly heterogeneous from a homogeneous reaction. DMFc is sparingly soluble in the aqueous phase and one can consider that the reaction may take place in 1,2-DCE. Since the oxidized $DMFc^+$ is present in the organic phase, the reduction of the protons must be accompanied by a transfer of the lipophilic anion TB^- from the aqueous to the organic phase to maintain the electroneutrality. Indeed, aqueous TB^- is lipophilic enough to extract aqueous protons to the organic phase. In this case, the reaction can be written as

$$\begin{aligned} &H^+_{(w)} + TB^-_{(w)} \rightarrow H^+_{(DCE)} + TB^-_{(DCE)} \\ &DMFc_{(DCE)} + H^+_{(DCE)} + TB^-_{(DCE)} \xrightarrow{MoS_2,DCE} DMFc^+_{(DCE)} \\ &\qquad + TB^-_{(DCE)} + \frac{1}{2}H_{2(g)} \end{aligned} \tag{6}$$

It cannot be ruled out that the reaction occurs in the aqueous phase, although the solubility of DMFc is small. In this case, we have

$$\begin{aligned} &DMFc_{(DCE)} \rightarrow DMFc_{(w)} \\ &DMFc_{(w)} + H^+_{(w)} + TB^-_{(w)} \xrightarrow{MoS_2} DMFc^+_{(DCE)} \\ &\qquad + TB^-_{(DCE)} + \frac{1}{2}H_{2(g)} \end{aligned} \tag{7}$$

In both cases, the driving force for the reaction is the same. Indeed for the organic pathway, we have

$$\begin{aligned} \Delta G^0_{HER}/F = &\left[E^0_{DMFc^+/DMFc}\right]^{DCE}_{SHE} - \left[E^0_{H^+/1/2H_2}\right]^{DCE}_{SHE} \\ &+ \Delta G^{0,w\rightarrow DCE}_{tr,TB^-}/F + \Delta G^{0,w\rightarrow DCE}_{tr,H^+}/F \end{aligned} \tag{8}$$

with the redox potential in the organic phase being defined by

$$\left[E^0_{H^+/1/2H_2}\right]^{w}_{SHE} = \left[E^0_{H^+/1/2H_2}\right]^{DCE}_{SHE} - \Delta G^{0,w\rightarrow DCE}_{tr,H^+}/F \tag{9}$$

which gives

$$\begin{aligned} \Delta G^0_{HER}/F = &\left[E^0_{DMFc^+/DMFc}\right]^{DCE}_{SHE} - \left[E^0_{H^+/1/2H_2}\right]^{w}_{SHE} \\ &+ \Delta G^{0,w\rightarrow DCE}_{tr,TB^-}/F \end{aligned} \tag{10}$$

For the aqueous pathway, we have

$$\begin{aligned} \Delta G^0_{HER}/F = &\left[E^0_{DMFc^+/DMFc}\right]^{w}_{SHE} - \left[E^0_{H^+/1/2H_2}\right]^{w}_{SHE} - \Delta G^{0,w\rightarrow DCE}_{tr,DMFc} \\ &+ \Delta G^{0,w\rightarrow DCE}_{tr,TB^-}/F + \Delta G^{0,w\rightarrow DCE}_{tr,DMFc^+}/F \end{aligned} \tag{11}$$

With the redox potential of DMFc in water being related to that in the organic phase by

$$\begin{aligned} \left[E^0_{DMFc^+/DMFc}\right]^{w}_{SHE} = &\left[E^0_{DMFc^+/DMFc}\right]^{DCE}_{SHE} - \Delta G^{0,w\rightarrow DCE}_{tr,DMFc^+}/F \\ &+ \Delta G^{0,w\rightarrow DCE}_{tr,DMFc} \end{aligned} \tag{12}$$

we recover eqn (10). The standard Gibbs energies of transfer of TB^- are equal to -70 kJ mol^{-1} and the driving force is about -65 kJ mol^{-1}.

These thermodynamic considerations show that both the interfacial and the bulk reactions are exergonic and that both bulk reactions have a higher driving force than the heterogeneous interfacial one. It is therefore likely that proton reduction by DMFc and catalysis by MoS_2 in mechanically stirred systems can occur both homogeneously and heterogeneously.

Conclusions

MoS_2 has been shown to be an efficient catalyst for the reduction of aqueous protons by organic electron donors such as decamethylferrocene. This work opens the way for the investigation of other triphasic systems for the production of hydrogen without using noble metals. If this reaction is coupled to a photosystem, it may provide new biomimetic strategies for water splitting at soft interfaces.

Notes and references

1 H. H. Girault, in *Electroanalytical Chemistry, A series of Advances*, ed. A. J. Bard and C. G. Zoski, CRC Press, Boca Raton, 1st edn, 2010, vol. 23, ch. 1, pp. 1–104.
2 I. Hatay, B. Su, F. Li, M. A. Méndez, T. Khoury, C. P. Gros, J.-M. Barbe, M. Ersoz, Z. Samec and H. H. Girault, *J. Am. Chem. Soc.*, 2009, **131**, 13453–13459.
3 R. Partovi-Nia, B. Su, F. Li, C. P. Gros, J.-M. Barbe, Z. Samec and H. H. Girault, *Chem.–Eur. J.*, 2009, **15**, 2335–2340.
4 B. Su, I. Hatay, A. n. Trojánek, Z. k. Samec, T. Khoury, C. P. Gros, J.-M. Barbe, A. Daina, P.-A. Carrupt and H. H. Girault, *J. Am. Chem. Soc.*, 2010, **132**, 2655–2662.
5 R. Partovi-Nia, B. Su, M. A. Méndez, B. Habermeyer, C. P. Gros, J.-M. Barbe, Z. Samec and H. H. Girault, *ChemPhysChem*, 2010, **11**, 2979–2984.
6 M. A. Mendez, R. Partovi-Nia, I. Hatay, B. Su, P. Ge, A. Olaya, N. Younan, M. Hojeij and H. H. Girault, *Phys. Chem. Chem. Phys.*, 2010, **12**, 15163–15171.
7 A. Trojánek, J. Langmaier, B. Su, H. H. Girault and Z. Samec, *Electrochem. Commun.*, 2009, **11**, 1940–1943.
8 I. Hatay, B. Su, M. A. Méndez, C. m. Corminboeuf, T. Khoury, C. P. Gros, M. l. Bourdillon, M. Meyer, J.-M. Barbe, M. Ersoz,

S. Záliš, Z. k. Samec and H. H. Girault, *J. Am. Chem. Soc.*, 2010, **132**, 13733–13741.
9 A. Trojánek, J. Langmaier and Z. Samec, *Electrochem. Commun.*, 2006, **8**, 475–481.
10 U. Koelle, P. P. Infelta and M. Graetzel, *Inorg. Chem.*, 1988, **27**, 879–883.
11 I. Hatay, B. Su, F. Li, R. Partovi-Nia, H. Vrubel, X. Hu, M. Ersoz and H. H. Girault, *Angew. Chem., Int. Ed.*, 2009, **48**, 5139–5142.
12 J. J. Nieminen, I. Hatay, P. Ge, M. A. Mendez, L. Murtomaki and H. H. Girault, *Chem. Commun.*, 2011, **47**, 5548–5550.
13 H. Tributsch and J. C. Bennett, *J. Electroanal. Chem. Interfacial Electrochem.*, 1977, **81**, 97–111.
14 A. Nidola and R. Schira, *Int. J. Hydrogen Energy*, 1986, **11**, 449–454.
15 A. Sobczynski, *J. Catal.*, 1991, **131**, 156–166.
16 T. F. Jaramillo, K. P. Jørgensen, J. Bonde, J. H. Nielsen, S. Horch and I. Chorkendorff, *Science*, 2007, **317**, 100–102.
17 J. Bonde, P. G. Moses, T. F. Jaramillo, J. K. Norskov and I. Chorkendorff, *Faraday Discuss.*, 2009, **140**, 219–231.
18 D. Merki, S. Fierro, H. Vrubel and X. Hu, *Chem. Sci.*, 2011, **2**, 1262–1267.
19 X. Zong, H. Yan, G. Wu, G. Ma, F. Wen, L. Wang and C. Li, *J. Am. Chem. Soc.*, 2008, **130**, 7176–7177.
20 A. Zahl, R. van Eldik, M. Matsumoto and T. W. Swaddle, *Inorg. Chem.*, 2003, **42**, 3718–3722.
21 B. Su, J.-P. Abid, D. J. Fermín, H. H. Girault, H. Hoffmannová, P. Krtil and Z. Samec, *J. Am. Chem. Soc.*, 2003, **126**, 915–919.
22 T. Wandlowski, V. Marecek and Z. Samec, *Electrochim. Acta*, 1990, **35**, 1173–1175.
23 N. Eugster, D. J. Fermín and H. H. Girault, *J. Phys. Chem. B*, 2002, **106**, 3428–3433.
24 B. Hinnemann, P. G. Moses, J. Bonde, K. P. Jørgensen, J. H. Nielsen, S. Horch, I. Chorkendorff and J. K. Nørskov, *J. Am. Chem. Soc.*, 2005, **127**, 5308–5309.
25 B. Su, R. P. Nia, F. Li, M. Hojeij, M. Prudent, C. Corminboeuf, Z. Samec and H. H. Girault, *Angew. Chem., Int. Ed.*, 2008, **47**, 4675–4678.
26 M. E. Flatte, A. A. Kornyshev and M. Urbakh, *Faraday Discuss.*, 2009, **143**, 109–115.